



Heat and Mass Transfer with reference to Aerodynamics

Menka Yadav¹ and Santosh Kumar Yadav²

¹Research Scholar, J.J.T. University, Rajasthan, India

²Director (A&R), J.J.T. University, Rajasthan, India

(Corresponding author: Menka Yadav)

(Received 19 March, 2017 Accepted 28 April, 2017)

(Published by Research Trend, Website: www.researchtrend.net)

ABSTRACT: Aerodynamic heating produces during passage of high speed aircraft and greatest at high speed and in lower atmosphere, highly dependent on design of vehicle. It plays important role in supersonic and hypersonic so the nose and wing leading edges should be blunt not sharp. Important information regarding heat and mass transfer is provided by the impinging jet. To characterize heat and mass transfer Nusselt number (N_u) and Schmidt number (S_c) are used. Total aerodynamic heating comprises of convective and radiative heating. To get rid of massive heat accumulation, heat sinks, ablation and radiative cooling is employed. Mass transfer from flat surfaces depends on Reynold and Schmidt number.

Keywords: Blunt shape, Impinging jet, Nusselt number, Reynold number, Schmidt number and Slender body.

I. INTRODUCTION

Basic unit of heat and mass exchanger are ducts and to make contacts between gases, solid and liquid, interface is provided by ducts. Aerodynamic heating is the heating of a solid body produced when it passes through air with very high speed (or by the passage of air past a test object in a wind tunnel), where its K.E. converted into heat by skin friction on the surface of object which in turn depends on the viscosity and speed of the air. It is highly related to meteors, reentry vehicles, and the design of high speed aircraft. While object passing through air at high speed, K.E. converts into heat through compression and friction. At lower speed, if air is cooler, then object lose heat to the air. The combined temperature effect of heat from the air and passage through it is called stagnation temperature and the actual temperature is called recovery temperature. Boundary layer slow down via a non-isentropic process due to viscous dissipative effects to neighbouring sub layers. Conduction of heat takes place into the surface material from the higher temperature air. Consequently, temperature of material increases and a loss of energy from the flow. It is ensured by forced convection that other material replenishes the gases that have cooled to continue the process. As the speed of flow increases, stagnation and recovery temperature increases. Furthermore, total thermal loading of the object is a function of recovery temperature and the mass flow rate.

Aerodynamic heating is greatest at high speed and in the lower atmosphere where the density is greater, also increase with the speed of vehicle. Supersonic flow is the fluid motion in which Mach number is greater than unity relative to the sonic speed in the same medium.

Practical problems arises in construction of steam turbines, gas turbines, high pressure turbocompressors and in wind tunnel. Flow at high supersonic speed is known as hypersonic flows. The temperature of gas rises very high when a body flies at hypersonic speed. Increase in temperature takes place due to highly compressed gas in front of nose and heat produced due to internal friction carried by the body. In hypersonic flow air properties changes at high temperature like excitation of internal degree of freedom, dissociation of gas molecules, chemical reactions (formation of nitric acid), excitation of electrons and ionization. At lowering the peak temperature leading edges, heating effects are greatest but if it remains at speed then the whole vehicle heats up to a stabilized temperature. Turbulent flow is described by random fluctuations in quantities like velocity temperature etc. In absence of such fluctuations, flow is known as laminar. At transition, Reynold no. laminar flow turns into turbulent flow.

At subsonic speed its effects are minimal but at supersonic speeds above $M 2.2$ it dictates the design/materials of the vehicle structure and internal systems.

A. Aircraft and Reentry vehicles

Aerodynamic heating concerns with supersonic and hypersonic. The SR-71 used titanium skin panels painted black to reduce the temperature and corrugated to accommodate expansion. Liquid cooling of the leading edges is also used in some designs for hypersonic missiles (usually the fuel en route to the engine). For Mach 10 temp. several design iterations are used, for sprint missile heat shield.

To get rid of massive heat accumulation, three approaches are used for thermal protection systems as Heat sinks, Ablation, Radiative cooling.

Heat sinks are extramaterial used to absorb the heat by lowering the peak temperature can be lowered by increasing the volume of material. Carbon and ceramics have very high latent heat of fusion. During vaporization, these materials soak up large amount of heat energy. If the Vehicle's surface is coated with these material, then vehicle can be protected. The melting process can be termed as ablation. Radiative cooling is the process of reducing equilibrium temp., by emitting heat energy before absorbing the vehicle's structure.

Immense heat is created by very high reentry speeds (greater than Mach 20) and it is sufficient to destroy vehicle so special techniques are used. To produce a stand-off bow shock blunt shape is given such as used on Mercury, Gemini and Apollo. It results, most of heat dissipation transfer to surrounding air without transferring the vehicle structure. Moreover, at high temp., these vehicle's ablative material sublimate into gas. During sublimation process, thermal energy is absorbed from the aerodynamic heating and material is eroded as opposed to heating the capsule. The surface of the heat shield for the Mercury spacecraft had a coating of aluminium with glass fiber in many layers. As the temperature increases upto 1100°C (1400 K), layer would evaporate and take the heat with it. The spacecraft get heated but not harmfully, so on lower surface of space shuttle insulating tiles are used to absorb and radiate heat vehicle preventing conduction to the aluminium airframe.

Cooling fin is also used to transfer heat from a solid to an ambient fluid for cooling purpose often exhibit slender geometries. Their dimension in the conductive heat transfer are larger than in directions transverse to it (fins or needles). Thermal energy balance is allowed by geometrical property of the fin to be formulated in a quasi one-dimensional form, where coordinates of conductive heat transport are geometrical properties of fin and temperature. Improving design tools with respect to flight experiment could be helpful in the development of aerodynamics.

Aerodynamic heating becomes severe at hypersonic speed so the nose and leading edges should be blunt not sharp, otherwise vehicle can be destroyed by aerodynamic heating. The unfortunate example of this type of destruction occurred during liftoff of the space shuttle Columbia on February 1, 2003. During launch many thermal protection tiles near the leading edge of the left wing get damaged by debris. It permitted the penetration of hot gases into surface and damage the internal wing structure.

B. Impinging Jet Heat Transfer

Impingement jets provides information regarding transfer of heat and mass in an efficient way in many industrial

applications. Large amount of heat and mass can be transferred in an effective way if flow released against a surface. Heat transfer process used in heating of optical surfaces, cooling of electronic components, turbine components and critical machinery structures and in aeronautical, chemical, civil, electrical, metallic and metallurgical engineering. Drying and removal of small surface particulate are applications of typical mass transfer. In practical applications, if order of magnitude of Reynold number is greater than boundary layer thickness in stagnation zone becomes $\frac{1}{100^{\text{th}}}$ of nozzle diameter. Jet

has finite breadth and it exchanges momentum with surrounding, then accelerated stagnation flow converts into decelerated wall jet flow. In stagnation zone, boundary layer becomes laminar due to stabilizing effect of acceleration. In comparison to other heat and mass transfer arrangements, which do not involve phase change, efficient use of fluid and high transfer rates are offered by jet impingement device. Due to very thin impingement boundary layer heat transfer coefficients are three times higher at a given maximum flow speed than conventional convection cooling by confined flow parallel to the cooled surface. Multiple jets can be used for more uniform coverage over large surfaces. It also offers a compact hardware arrangements.

To characterize heat transfer at the target surface, Nusselt number (N_u) and the mass transfer from the surface with a Schmidt number (S_c) are used. For device performance assessment and design efficiency, these values are tracked vs. jet flow per unit area or vs. the power required to supply the flow.

C. Impinging Jet Regions

The flow of a submerged impinging jet passes through different regions as shown in Fig. 1. The jet comes out from a nozzle with a velocity and temperature profile, and the turbulence characteristics depends upon the upstream flow. For a tube nozzle, the flow develops into the parabolic velocity profile. A round jet with an axisymmetric flow profile or a slot jet, a long thin jet with a two-dimensional flow profile is used in typical jet nozzles. It behaves as a free submerged jet when it passes far from impingement surface. At the edges of jet velocity gradient create a shearing at the edges, which allows the transfer of momentum laterally outward and raises the jet mass flow. During this process energy is lost by jet and the velocity profile becomes wide in spatial extent and decreases in magnitude along jet sides. Due to momentum transfer shearing layer remains unaffected. If nozzle is at two diameters (2D) from the target, then free jet region may not exist.

Region of core decay forms when shearing layer expands inside the center of jet prior to reaching the target.

The axial position at which centralline flow dynamic pressure attains 95% of its original value, known as the end of one region.

In the decay jet, the radial velocity profile resembles to Gaussian curve and axial velocity component decreases in central part. In stagnation region or deceleration region, as the flow approaches the wall, it loses axial velocity. The higher static pressure on and above the wall is created by the flow. In the deceleration region, high normal and shear stresses is experienced by the non-uniform turning flow by which local transport properties are affected to a great extent. For round jets stagnation region extends 1.2 nozzle diameters above the wall. After the flow turns the core of the wall jet may accelerate due to conservation of momentum.

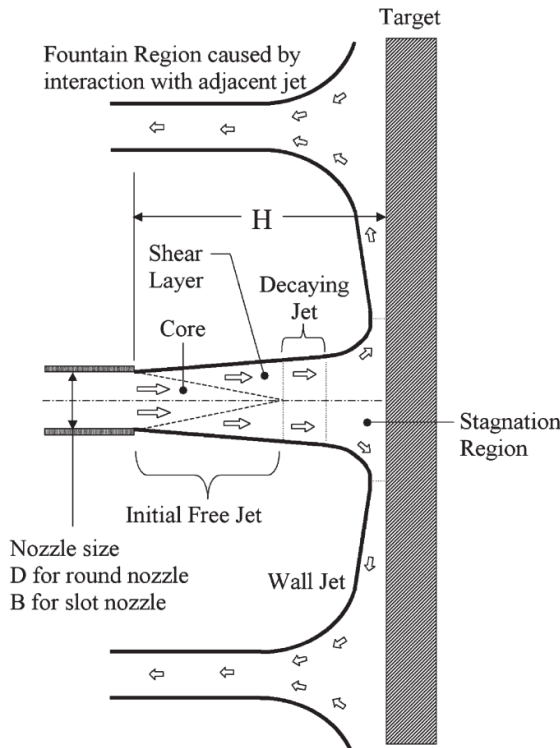


Fig. 1. The flow regions of an impinging jet.

Non dimensional Heat and Mass Transfer Coefficients:

Nusselt (N_u) no. is a major parameter to evaluate heat transfer coefficient

$$N_u = hD_n / K_c$$

where h is the convective heat transfer coefficient and can be defined as

$$h = \frac{-K_c \frac{\partial T}{\partial \bar{n}}}{T_{ojet} - T_{wall}}$$

where $\frac{\partial T}{\partial \bar{n}}$ provides the temperature gradient

component normal to the wall. Nusselt number is independent of target characteristics. T_{ojet} is the jet temperature for adiabatic wall temperature of the deceleration jet flow, a factor of vital importance at increasing Mach numbers. Amount of K.E. is transferred into and retained in thermal form as the jet slows down, known as non-dimensional recovery factor.

$$\text{recovery factor} = \frac{T_{wall} - T_{ojet}}{U_{jet}^2 / 2C_p}$$

Experiments shows that the temperature recovery factor varies from 70% to 100% of the full theoretical recovery with lowered recoveries in the stagnation region of a low H/D jet ($H/D = 2$) and 100% elevated stagnation region recoveries for jet with $H/D = 6$ and higher.

Rate of mass transfer can be evaluated by non-dimensional Sherwood number as

$$Sh = K_i D / D_i$$

$$k_i = D_i \left[\frac{\partial C}{\partial n} \right] / [C_{obj} - C_{wall}]$$

where $\frac{\partial C}{\partial n}$ provides the mass concentration gradient

component normal to the wall. Spatial distribution of concentration forms similar pattern as the temperature with sufficiently low mass concentration. Heat and mass transfer can be related via equation given below

$$N_u / Sh = \left(\frac{P_r}{S_c} \right)^{0.4}$$

The non-dimensional parameters which describe the impinging jet heat transfer problem comprises properties such as Prandtl number P_r (ratio of fluid thermal diffusivity to viscosity) and the following:

- H/D : Nozzle height to nozzle diameter ratio
- r/D : Non-dimensional radial position from the center of the jet.
- Z/D : non-dimensional vertical position measured from the wall.
- T_u : non-dimensional turbulence intensity generally evaluated at the nozzle.
- Re_0 : Reynolds number $U_0 D / \nu$;
- M : Mach number (flow of speed / speed of sound in the fluid).
- P_{jet}/D : Jet center to center spacing (pitch) to diameter ratio, for multiple jets.
- A_f : Free area

f : relative nozzle area

Flow exist at the nozzle is considered as the reference location while evaluating the fluid properties. Using position characteristics we can calculate fluid temperature average flow speed, viscosity and length scale D. Diameter D can be replaced by the slot width B in slot jet. Nature of the target and the field source are the two parameters necessary for geometry and flow conditions in impinging jet. When pressure drop associated with delivering and exhausting the flow is very-2 small, then the design goal is to extract cooling from a given air mass flow. The jet emerges at a high Mach number at high pressure ratios. If the flow exists the nozzle as an under expanded supersonic jet, then jet forms complex interacting shock patterns and a recirculation "bubble" directly below the jet, which can decreases heat transfer. Moreover, overall device performance is affected by the impingement device design.

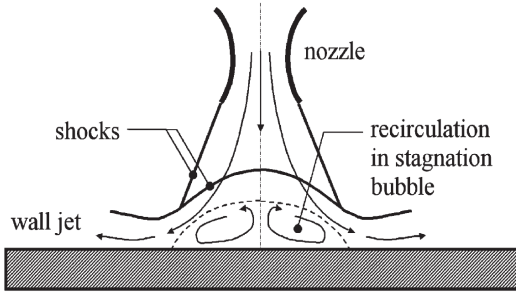


Fig. 2. Supersonic jet flow pattern.

Turbulence Generation and Effects

Jet behaviour is described by its Reynold no. $Re = U_0 D / \nu$ where U_0 is initial flow speed, ν is viscosity and D is nozzle exist diameter. Laminar flow properties are shown by flow field at $Re < 100$ but at $Re > 3000$, flow field shows turbulent properties. Transition region lies in between $1000 < Re < 3000$ Turbulence affects greatly the heat and mass transfer rates. For e.g., an isolated round jet at $Re = 2000$, $Pr = 0.7$, $H/D = 6$ delivers an average Nu of 19 over a circular target spanning six jet diameters, but at $Re = 100,000$ the average Nu on the same target spacing value of Nu lies in the range of 2 –20. In the relation of Nusselt number and Reynold number $Nu \propto Re^b$, the exponent b ranges $b = 0.5$ for low-speed flows with a low-turbulence wall jet, upto $b = 0.85$ for high Re flows with a turbulence-dominated wall jet.

For a underexpanded supersonic jet at $Re = (1.028) \times 10^6$ local Nu values may be as high as 1700. Reynold number varies from 4000 to 80,000 in case of gas jet installations and H/D can vary from 2 to 12.

As H decreases, value of Nu increases, so designer prefer to select smallest tolerable H value, effects of existing flow, physical constraints, manufacturing capabilities and then selects nozzle size.

Jet diameters ranges from 5-30 mm for large scale industrial applications and from 0.2 to 2 mm for small-scale turbomachinery application.

At low Mach number modelling of turbulent flow is defined by the mass, momentum and energy conservation equation :

$$\frac{\partial \bar{u}_i}{\partial x_i} = 0$$

$$\rho \frac{\partial \bar{u}_i}{\partial t} + \rho \bar{u}_i \frac{\partial \bar{u}_j}{\partial x_j} = -\frac{\partial \bar{p}}{\partial x_i} + \frac{\partial \sigma_{ij}}{\partial x_j} + \frac{\partial \tau_{ij}}{\partial x_j}$$

$$\rho \frac{\partial \bar{u}_i}{\partial t} + \rho \bar{u}_i \frac{\partial \bar{u}_j}{\partial x_j} = -\frac{\partial \bar{p}}{\partial x_i} + \frac{\partial}{\partial x_j} \left[\mu \left(\frac{\partial \bar{u}_i}{\partial x_j} + \frac{\partial \bar{u}_j}{\partial x_i} \right) + \frac{\partial}{\partial x_i} (-\rho u_i u_j) \right]$$

(Alternate form)

$$\rho C_p \frac{\partial \bar{T}}{\partial t} + \rho C_p \bar{u}_j \frac{\partial \bar{T}}{\partial x_j} = \sigma_{ij} \frac{\partial \bar{u}_i}{\partial x_j} + \frac{\partial}{\partial x_j} \left(\frac{\mu C_p \partial \bar{T}}{P_r \partial x_j} \right) +$$

$$\frac{\partial}{\partial x_j} (-\rho C_p \overline{u_j T'}) + \mu \left(\frac{\partial u'_i}{\partial x_j} + \frac{\partial u'_j}{\partial x_i} \right) \frac{\partial u'_i}{\partial x_j}$$

$$\sigma_{ij} = \mu \left(\frac{\partial \bar{u}_i}{\partial x_j} + \frac{\partial \bar{u}_j}{\partial x_i} \right)$$

$$\tau_{ij} = -\rho \overline{u'_i u'_j}$$

where an overbar above a single letter represents a time-average term and prime symbol represent fluctuating values and a large overbar represent a correlation. The time variant momentum equation gives the conservative transport equation for Reynolds stresses for an incompressible field.

$$\frac{\partial \tau_{ij}}{\partial t} + \bar{u}_k \frac{\partial \tau_{ij}}{\partial x_k} = \left[-\tau_{ik} \frac{\partial \bar{u}_j}{\partial x_k} - \tau_{jk} \frac{\partial \bar{u}_i}{\partial x_k} \right] + \left[\frac{\rho'}{\rho} \left(\frac{\partial u'_j}{\partial x_j} + \frac{\partial u'_i}{\partial x_i} \right) \right] +$$

$$\left[\frac{\partial}{\partial x_{jk}} \left(-u'_i u'_j u'_k - \frac{\rho'}{\rho} \{ u'_i \delta_{jk} + u'_j \delta_{ik} \} \right) \right] + \left[-2\nu \frac{\partial u'_i}{\partial x_k} \frac{\partial u'_j}{\partial x_k} \right] + \left[\nu \frac{\partial^2 \tau_{ij}}{\partial x_k \partial x_k} \right]$$

$\frac{\partial \tau_{ij}}{\partial t} + \bar{u}_k \frac{\partial \tau_{ij}}{\partial x_k}$ represent convective transport of Reynold stress

$$\tau_{ik} \frac{\partial \bar{u}_j}{\partial x_k} + \tau_{jk} \frac{\partial \bar{u}_i}{\partial x_k}$$

measures turbulent production of Reynold stresses.

$\frac{p'}{\rho} \left(\frac{\partial u'_i}{\partial x_j} + \frac{\partial u'_j}{\partial x_i} \right)$ measures the contribution of the pressure-strain rate correlation to Reynold stresses.

The term $\frac{\partial}{\partial x_k} \left[-\overline{u'_i u'_j u'_k} - \frac{p'}{\rho} \{ u'_j \delta_{jk} + u'_i \delta_{jk} \} \right]$ gives the effect of the gradient of turbulent diffusion.

$-2\nu \frac{\partial u'_i \partial u'_j}{\partial x_i \partial x_k}$ represent the effects of turbulent dissipation.

$\nu \frac{\partial^2 T_{ij}}{\partial x_k \partial x_k}$ represent the effects of molecular diffusion.

Intensity of turbulent flow field is given by the specific turbulent K.E. k . Downstream flow and heat transfer characteristics are affected by the steady time-averaged nozzle-velocity profile and fluctuations in the velocity over time. Turbulent fluctuations helps to understand the performance of impinging jets.

Aerodynamic heating depends on the design of vehicle also. Laminar flow produces less heating than turbulent flow so to minimize it, focus is to maintain the boundary layer flow on the vehicle's surface. At the beginning reentry vehicle posses large amount of P.E. due to its high altitude and large amount of K.E. due to high velocity. But when the vehicle lift off to earth, it has no K.E. & P.E. This shows that the huge amount of energy is imparted to heating the body and the airflow around the body. If a major portion of energy is transferred to the air, then less amount of energy will be transferred in vehicle heating. Heat transfer rate to the airflow can be increased by creating a stronger shock wave at the nose which is turn can be achieved using blunt nose body. Through mode of conduction energy is transferred from the hot shock layer to the surfaces.

Convective heating is given by,

$$q_c = -k \left(\frac{\partial T}{\partial n} \right)$$

where $\frac{\partial T}{\partial n}$ represents temperature gradient and it is property of flow field.

It is important mode of heat transfer for reentry velocities. At high temp., mode of heat transfer is radiation. Total aerodynamic heating can be expressed as $q = q_c + q_r$ where q_c and q_r are convective heating and radiative heating respectively.

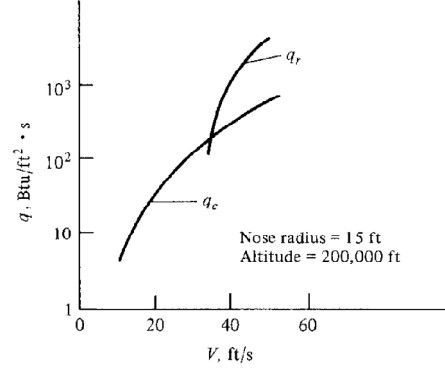


Fig. 3. Convective and radiative heating rates of a blunt reentry vehicle as a function of flight velocity.

Aerodynamic heating in hypersonic flow:

Heat transfer coefficient (Stanton number) can be defined as

$$C_H = \frac{\dot{q}_w}{\rho_e u_e (h_{aw} - h_w)} \quad (7)$$

where \dot{q}_w represents heat transfer rate per unit area on body surface at a given point

ρ_e = local density at the edge of boundary

u_e = local velocity at the edge of boundary

h_w = enthalpy of the gas at wall.

h_{aw} = adiabatic wall enthalpy

At zero angle of attack consider the hypersonic flow ignoring viscous interaction effect where $\rho_e = \rho_w$ and $u_e = u_\infty$.

T_{aw} is nearly 12 percent less than the total temperature in free stream at high Mach number laminar flow over a flat plate. If $T_{aw} \approx T_0$ then from equation (1)

$$h_{aw} \approx h_a \quad (2)$$

where h_0 represents the total enthalpy of the freestream, which can be expressed as

$$h_0 = h_\infty + \frac{V_\infty^2}{2} \quad (3)$$

V_∞ is very large at hypersonic speed.

Air is comparatively cool at far ahead of the vehicle. Therefore $h_\infty = C_p T_\infty$ is small. So at high speeds, from equation (3).

$$h_0 \approx \frac{V_\infty^2}{2} \quad (4)$$

At high Mach number surface temperature of the plate is smaller than the total temperature. Hence we made approximation that $h_0 \gg h_w$ (5)

We can write from the above mentioned equations,

$$h_{aw} - h_w \approx h_0 - h_w \approx h_0 \approx \frac{V_\infty^2}{2} \quad (6)$$

So for a flat plate, equation can be written as –

$$C_H = \frac{\dot{q}_w}{\rho_\infty V_\infty (h_{aw} - h_w)}$$

Using equation (6)

$$C_H \approx \frac{\dot{q}_w}{\rho_\infty V_\infty (V_\infty^2 / 2)}$$

$$\text{or} \quad \dot{q}_w \approx \frac{1}{2} \rho_\infty V_\infty^3 C_H \quad (7)$$

It shows that aerodynamic heating depends on the cube of velocity but aerodynamic drag varies with square of velocity. It shows that aerodynamic heating becomes a dominant aspect of hypersonic vehicle design at very high velocities. It connects the aerodynamic heating with hypersonic flow.

Quantitative Explanation of blunt vs. Slender bodies in Hypersonic flow

Stanton number \bar{C}_H for total heat transfer to the vehicle per unit time is

$$\bar{C}_H = \frac{dQ/dt}{\rho_\infty V_\infty (h_0 - h_w) S} \quad (8)$$

where S represents reference area and making use of approximation equation (7) can be written as

$$\frac{dQ}{dt} = \frac{1}{2} \rho_\infty V_\infty^3 S \bar{C}_H \quad (9)$$

For laminar flow Reynold's analogy can be expressed as,

$$\frac{C_H}{C_f} = \frac{1}{2} P_r^{-2/3} \quad (10)$$

where C_f denotes local skin friction coefficient and P_r denotes Prandtl number.

If $P_r = 1$, then Reynold analogy can be written as

$$\frac{\bar{C}_H}{C_f} = \frac{1}{2} \quad (11)$$

Substituting equation (11) into (10) we get,

$$\frac{dQ}{dt} = \frac{1}{4} \rho_\infty V_\infty^3 S C_f \quad (12)$$

In case of hypersonic vehicle entry at very high Mach number in space, aerodynamic drag slows down the vehicle.

According to Newton's second law,

$$F = D = -m \frac{dV_\infty}{dt} \quad (13)$$

where m represents mass of vehicle and minus sign represents deceleration of vehicle:

From above equation,

$$\frac{dV_\infty}{dt} = -\frac{D}{m} = -\frac{1}{2m} \rho_\infty V_\infty^2 S C_D \quad (14)$$

where C_D denotes vehicle's drag coefficient and $\frac{dQ}{dt}$

can be written as $\left(\frac{dQ}{dV_\infty}\right)\left(\frac{dV_\infty}{dt}\right)$

Then

$$\frac{dQ}{dt} = \frac{dQ}{dV_\infty} \left(-\frac{1}{2m} \rho_\infty V_\infty^2 S C_D\right) \quad (15)$$

From (12) and (15)

$$\frac{dQ}{dV_\infty} \left(-\frac{1}{2m} \rho_\infty V_\infty^2 S C_D\right) = \frac{1}{4} \rho_\infty V_\infty^3 S C_f$$

$$\text{or} \quad \frac{dQ}{dV_\infty} = -\frac{1}{2} m V_\infty \frac{C_f}{C_D}$$

$$dQ = -\frac{1}{2} m \frac{C_f}{C_D} \frac{dV_\infty^2}{2} \quad (16)$$

Integrating from beginning of entry to the end, we have Q total

$$\int_0^{Q_{\text{total}}} dQ = -\frac{1}{2} \frac{C_f}{C_D} \int_{V_E}^0 d\left(\frac{V_\infty^2}{2}\right)$$

$$\text{or} \quad Q_{\text{total}} = \frac{1}{2} \frac{C_f}{C_D} \left(\frac{1}{2} m V_E^2\right) \quad (17)$$

Equation (17) gives the total heat input and two major conclusions can be drawn from it.

(i) Total input heat Q_{total} varies directly with $\frac{1}{2} m V_E^2$ (K.E. of vehicle)

(ii) It is also directly proportional to $\frac{C_f}{C_D}$ where C_f and

C_D represents skin friction drag and total drag respectively.

(iii) Aerodynamic drag on a vehicle is, $C_D = C_{D_p} + C_f$

where C_{D_p} is pressure drag coefficient

and C_f is skin friction coefficient.

To minimize total aerodynamic heating in equation (17), it is necessary to minimize,

$$\frac{C_f}{C_{D_p} + C_f}$$

Now consider the aerodynamic configuration as shown in fig given below,

$$\frac{C_f}{C_D} \approx 1 \text{ for slender body}$$

$$\frac{C_f}{C_D} \ll 1 \text{ for slunt body}$$

Reason being large skin friction for slender body and large pressure drag for blunt body.

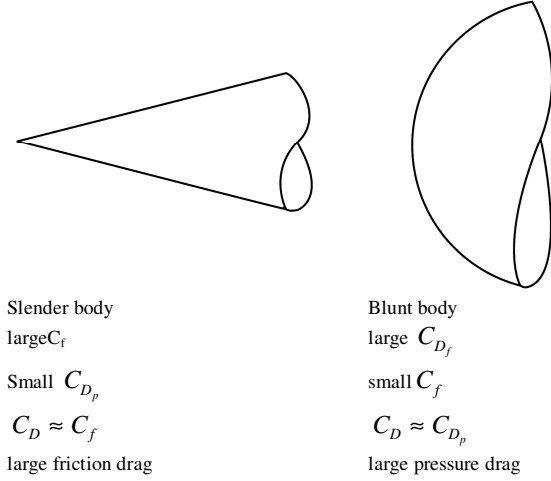


Fig. 4. Comparison of blunt and slender bodies.

Due to this reason all successful entry vehicles utilize rounded nose and rounded leading edge. For e.g. intercontinental ballistic missiles (ICBMs), Apollo lunar return capsule, space shuttle etc.

Aerodynamic heating for blunt shape can be calculated at the stagnation point. In hypersonic, maximum heat transfer takes place at this point. Relation between stagnation point and nose radius is given by

$$\dot{q}_w \propto \frac{1}{\sqrt{R}}$$

where R represent nose radius at stagnation.

It is clear that to reduce heating we must increase nose radius. Shock waves associated with blunt vehicles are detached and spread the heat of re-entry over a relatively large volume. At the surface of blunt vehicles, air flow tends to inhibit convective heat transfer, which lowers the heating rate for blunt vehicles. Streamlined vehicles have attached shock waves due to it temperature becomes very high at sharp tip, which is sufficient to melt most of the materials.

Mass Transfer

Mass transfer can be affected by Brownian in a flowing fluid and surface gradient in temperature arise diffusive mass flux. If mass is transported by equimolar diffusion, then different mixture components are transported into two directions across a steady balance surface in space with equal rate of moles. Therefore no. of moles in mixture do not change during transport process. Therefore mixture concentration is constant on two sides of the surface. In Non-Equimolar diffusion mixture

concentration may vary in time and space, even in an isothermal system. Convective mass flux may arise due to inertial impaction, body force actions such as gravity, electrical and magnetic forces, lift force, particle inertia interaction and fluid turbulence field in homogeneity. In convective mass transfer product of conductance and driving force is known as total mass flux. In Turbulent boundary layer convective mass transfer product of boundary layer, flux of small particles can be obtained by integrating the modified Fick's law of diffusion,

$$J = -(D_B + D_f) \frac{dc}{dy}$$

where D_B denotes Brownian diffusivity.

and D_f denotes turbulent diffusivity and $\frac{dc}{dy}$ is concentration gradient

Mass Transfer from flat Surface

Consider a flat plate in fluid flow parallel to its surface and assumes that material properties are independent of composition take constant pressure and density throughout the flow field. Furthermore velocity field v is divergence free and no chemical reactions there.

In steady laminar flow, Sherwood number for forced convective mass transfer across a flat plate is given by

$$Sh = 0.332 \sqrt{R_{e_x}} S_c^{1/3}$$

where $R_{e_x} = U_{\infty} x / \nu$

and symbols have their usual meanings.

Value of ratio of thicknesses of the dynamic to concentration boundary layers is determined by $\sqrt{S_c}$. Small value of S_c represents thicker concentration boundary layer at a given position x along the plate. Consequently flow velocity is assumed constant, velocity ratio along a flat plate is determined by the Blasius solution of boundary layer problem.

Concentration profile is given by

$$\left. \frac{\rho_i - \rho_{i,w}}{\rho_{i,\infty} - \rho_{i,w}} \right|_{S_c \rightarrow 0} = \frac{\int_0^{\eta_r} \exp(-Sc\tilde{\eta}_r^2/4) d\tilde{\eta}_r}{\int_0^{\infty} \exp(-Sc\eta_r^2/4) d\eta_r}$$

In laminar field flow, non-dimensional concentration profile along flat plate for small S_c is given by

$$\left. \frac{\rho_i - \rho_{i,w}}{\rho_{i,\infty} - \rho_{i,w}} \right|_{S_c \rightarrow 0} = \frac{2}{\sqrt{\pi}} \int_0^{\xi} e^{-\xi^2} .d\xi = erf\left(\frac{\sqrt{S_c} \eta_r}{2}\right)$$

where erf represents error function.

The corresponding Sherwood no. is

$$\begin{aligned} Sh|_{Sc \rightarrow 0} &= \left. \frac{\partial \rho_i^*}{\partial y^*} \right|_{y^*=0} = \sqrt{\frac{U_\infty x}{\nu}} \left. \frac{d\rho_j^*}{d\eta_r} \right|_{\eta_r=0} \\ &= \sqrt{\frac{U_\infty x}{\nu}} \sqrt{\frac{S_c}{\pi}} \end{aligned}$$

It can be further written as

$$Sh|_{Sc \rightarrow 0} = 0.5642 \sqrt{R_x x} S_c^{1/2}$$

The above equation shows how Sherwood number depends on the Schmidt number.

Large Schmidt number means thinner concentration boundary layer than dynamic boundary layer. At large Schmidt number (S_c), sherwood number is given by

$$Sh|_{S_c \rightarrow 0} = 0.3387 \sqrt{R_x x} S_c^{1/3}$$

This relation shows dependency of Sherwood number on Reynold and Schmidt number.

Fluid particles may assume surface shapes it different from spherical equations derived for (Nusselt and) Sherwood numbers of diffusive (heat and) mass transfer across the surfaces are useful for transport process. Results developed by Frössling are useful for correlations of the Nusselt and Sherwood numbers. Correlations comprises of diffusive and corrective part and heat and mass transfer are analogous at low rates of mass transfer.

According to Frössling, Sherwood no. is given by

$$Sh = 2 + 0.552 R_x^{1/2} S_c^{1/3}$$

Constant 2 represents purely diffusive transfer from the spherical particle oscillation of gas bubble in liquid exhibit spheroidal equilibrium shapes.

II. CONCLUSION

In Aerodynamics, transfer of heat and mass gives insight of fluid flow with high speed objects. Blunt shape body helps to reduce heating and heat sinks, ablation and radiative cooling can be used for thermal protection. Minimization of pressure drag coefficient and skin friction coefficient reduces aerodynamic heating. Rate of mass transfer can be evaluated by non-dimensional Sherwood number. Nature of target and field source are important parameter in impinging jet.

REFERENCE

[1]. A. Bhandarker et. al, A Novel CFD method to estimate heat transfer coefficient for high speed flow 2016.
 [2]. A. Bhandarker et.al, A Novel CFD method to estimate heat transfer coefficient for high speed flow 2016.
 [3]. A.D. Kraus, A. Aziz, and J.R Welty, *Extended Surface Heat Transfer*, John Wiley & sons, New York, NY, USA, 2001
 [4]. Andrea de Lieto Vollaro et. al, CFD Analysis of Convective Heat Transfer Coefficient on External Surfaces of Buildings, 2015.

[5]. S.S Bhat and R.N. Govardhan, "Stall flutter of naca 0012 airfoil at low reynoldnumbers, " *Journal of Fluids and Structures*, May, 2013.
 [6]. B. Sunden et. al, *Heat and Mass Transfer*, 2014.
 [7]. B. Sunden et. al, *Heat and Mass Transfer*, 2014.
 [8]. Bird, R.B., Stewart, W.E. and Lightfoot, E.N., *Transport Phenomena* 2nd edition, Wiley, 2004.
 [9]. C.P. Kothandaraman, *Fundamentals of Heat and Mass Transfer*, 2006.
 [10]. Carslow, H.S., Jaeger, J.C.: *Conduction of Heat in Solids*, 2nd edn. Oxford Science Publications, Oxford (2005)
 [11]. Clarendon, Johnson, Haggie Smith, *Kelly : More than my share of it all*. Washington, D.C. Smithsonian Institution, Press, p. 141 ISBN 0874744911, 1985.
 [12]. D.Y. Shang, *Theory of Heat Transfer with Forced Convection Film Flows*, Springer Heidelberg, Dordrecht London, New York, 2011.
 [13]. D' Ambrosio D., "A study on shock Wave – Boundary Layer Interactions in High Speed Flows "4th European Symposium on Aerothermodynamics for Space Vehicles, October 2011.
 [14]. Davis J.P., Sturtevant, B., "Separation Length in High - Enthalpy Shock/ Boundary Layer Interaction", "Physics of Fluids, Vol. 12, No. 10, 2000.
 [15]. De Filippis F., Caristia S., Del Vecchio A., Purpura C., "The Scirocco PWT Facility Calibration Activities", 3rd international Symposium Atmospheric Re- entry Vehicle and Systems, Arcachon, France, March, 2003.
 [16]. Dharendra Kumar Dixit, *Heat and Mass Transfer*, 2016.
 [17]. Dharendra Kumar Dixit, *Heat and Mass Transfer*, 2016.
 [18]. Di Clemente M., Marini M., Schettino a, "Shock Wave Boundary Layer Interactions in SCIROCCO Plasma Wind Tunnel, East –West High Speed Flows Conference, Pechino, October 2005
 [19]. Di Clemente M., MARINI M., Schettino A, "Shock Wave Boundary Layer Interaction in EXPERT Flight Conditions and Scirocco PWT" , 13th AIAA/ CIRA International Space planes conference Capua , may 2005.
 [20]. E.L Cussler, *Diffusion Mass Transfer in Fluid systems*, 2013.
 [21]. Ethirajan Rathakrishan *Theoretical Aerodynamics*, First Edition, 2013, John Wiley & Sons Singapor Pvt. Ltd.
 [22]. F. Moukalled et.al, *The finite volume method in computational fluid dynamics*, 2016.
 [23]. Gunter Brenn, *Analytical Solution for Transport Process*, 2017.
 [24]. H.S. Carslow, J.C. Jaeger, *Conduction of Heat in Solids*, 2nd e dn. Oxford Science Publications, Oxford, 2005.
 [25]. Incropera, F.P., De Witt, D.P., Bergman, T.L., Lavine, A.S.: *Principles of Heat and Mass Transfer* 7thedn. Wiley, New York (2013).
 [26]. IzzetSachin and Adem Acir, *Numerical and experimental investigations of Lift and Drag Performances of NACA 0015 Wind Turbine Airfoil*, 2015.
 [27]. Kurt C. Rolle, *Heat and Mass Transfer*, 2016.
 [28]. Labs Bell, 1974, 9-17.
 [29]. R. Ben, Rich, Leo, Janes, *Skunk works: A personal memoir of my year at lockheedd*. Warner Books p. 218. ISBN 0751515035, 1994.